HHS Public Access

Author manuscript

Cell Host Microbe. Author manuscript; available in PMC 2024 January 11.

Published in final edited form as:

Cell Host Microbe. 2023 January 11; 31(1): 58–68.e5. doi:10.1016/j.chom.2022.11.002.

Widespread, human-associated redondoviruses infect the commensal protozoan *Entamoeba gingivalis*

Emma L. Keeler[1], **Carter Merenstein**[1], **Shantan Reddy**[1], **Louis J. Taylor**[2], **Ana G. Cobián-Güemes**[1], **Urvi Zankharia**[3], **Ronald G. Collman**[3,+], **Frederic D. Bushman**[1,+]

[1]Department of Microbiology, Perelman School of Medicine, University of Pennsylvania, Philadelphia, PA, USA

[2]Department of Microbiology and Immunology, University of Maryland School of Medicine, Baltimore, MD, USA

[3]Department of Medicine, Pulmonary, Allergy and Critical Care Division, Perelman School of Medicine, University of Pennsylvania, Philadelphia, PA, USA

SUMMARY

Redondoviruses are circular Rep-encoding single-stranded DNA (CRESS) viruses of high prevalence in healthy humans. Redondovirus abundance is increased in oro-respiratory samples from individuals with periodontitis, acute illness, and severe COVID-19. We investigated potential host cells supporting redondovirus replication in oro-respiratory samples and uncovered the oral amoeba *Entamoeba gingivalis* as a likely host. Redondoviruses are closely related to viruses of *Entamoeba* and contain reduced GC nucleotide content, consistent with *Entamoeba* hosts. Redondovirus and *E. gingivalis* co-occur in metagenomic data from oral disease and healthy human cohorts. When grown in xenic cultures with feeder bacteria, *E. gingivalis* was robustly positive for redondovirus RNA and DNA. A DNA proximity-ligation assay (Hi-C) on xenic culture cells showed enriched cross-linking of redondovirus and *Entamoeba* DNA, supporting *E. gingivalis* as the redondovirus host. While bacteria are established hosts for bacteriophages within the human virome, this work shows that eukaryotic commensals also contribute an abundant human-associated virus.

eTOC

Redondoviruses are widely present in human samples and are positively associated with several disease states. Keeler et al. report that redondoviruses are highly associated with *Entamoeba*

[+]joint corresponding authors: collmanr@pennmedicine.upenn.edu; bushman@pennmedicine.upenn.edu.

AUTHOR CONTRIBUTIONS

E.L.K., C.M., L.J.T, R.G.C. and F.D.B. designed the study. E.L.K., C.M., and L.J.T. carried out bioinformatic analysis. E.L.K., S.R., A.G.C.-G., and U.Z. carried out biochemical assays. All authors contributed to writing and editing the paper.

Lead contact: Frederic Bushman, bushman@pennmedicine.upenn.edu

DECLARATION OF INTERESTS

The authors declare no competing interests.

gingivalis and appear to replicate within this commensal amoeba. Thus, a commensal eukaryote can serve as a host for members of the human-associated virome.

Graphical Abstract

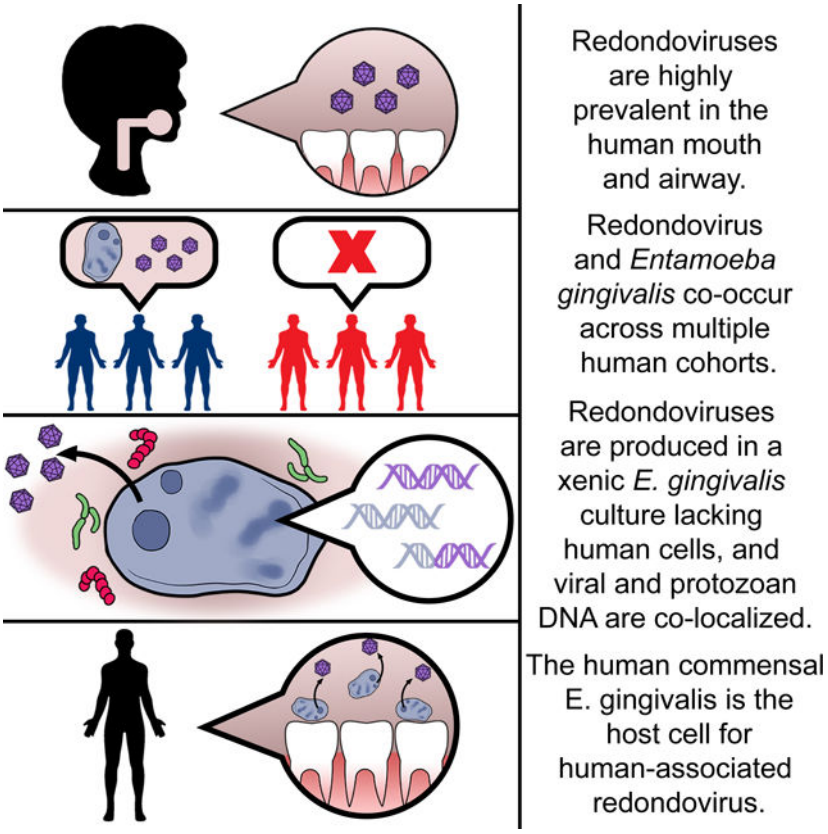

Keywords

Redondovirus; *Entamoeba gingivalis* ; CRESS virus; amoeba; virome; metagenomics; xenic culture

INTRODUCTION

Redondoviruses were first identified as metagenomic “dark matter” in studies of human respiratory virome samples[1,2]. In samples from lung transplant donors and recipients[1], a few virome sequence reads were initially found to align to porcine stool-associated circular virus 5, an uncharacterized viral genome identified in pig stool. Sequence assembly of the lung transplant samples yielded circular genomes of ~3 kb, with open reading frames (ORFs) distantly similar to capsid (Cap) and replication-associated (Rep) proteins of known CRESS viruses. The genomes recovered were ultimately classified into a newly-established family of viruses[3,4] termed *Redondoviridae*, (from “redondo”; Spanish for circle), with two species, *Vientovirus* and *Brisavirus* (from “viento” and “brisa”, Spanish for wind and breeze). Redondoviruses were further confirmed to be CRESS viruses by demonstrating that

purified Rep protein displayed the expected enzymatic activities in reconstructed reactions *in vitro*[5].

Use of redondovirus genome sequences as alignment targets to query published metagenomic data revealed that redondoviruses are present almost exclusively in human samples from the oro-respiratory tract. Redondoviruses were found in healthy people from North America, Africa, Europe, and Asia, with prevalence ranging from 2% to >80%, depending on cohort and sample type[1,2,5–7]. Redondoviruses were detected at elevated levels in subjects with multiple conditions, including lung transplant donors and recipients, febrile patients, and individuals with periodontitis, rheumatoid arthritis, inflammatory bowel disease, HIV infection, respiratory and oropharyngeal disease, critical illness, and COVID-19[1,6–9].

Here we investigated the cell type responsible for hosting redondovirus replication. Redondoviruses do not appear to replicate in prokaryotic cells because i) redondovirus genomes do not contain the Shine-Dalgarno translation initiation sequence that is characteristic of bacteriophages[10] and ii) redondovirus sequences are have not been found in arrays of prokaryotic CRISPR spacers[1,11,12]. Additionally, redondoviruses are phylogenetically distant from ssDNA bacteriophages (Figure S1A; Table S1). Given that redondoviruses have only been consistently detected in human samples, a simple model would be that redondoviruses replicate in human cells. However, evidence presented below identifies the human-associated amoeba *Entamoeba gingivalis* as the likely organism hosting redondovirus replication.

RESULTS

Redondovirus phylogeny and GC content are consistent with an *Entamoeba* host

A detailed phylogeny was recently proposed for CRESS viruses[3,13], including *Redondoviridae.* To investigate *Redondoviridae* further, we updated this phylogeny to include three CRESS virus families recently described in [13] and generated a maximum-likelihood tree of 441 Rep protein sequences (Table S1) from members of the *Cressdnaviricota* phylum, annotated with probable host organisms (Figure 1A). A close neighbor to the *Redondoviridae* family is *Naryaviridae*, whose members have recently been proposed to replicate in *Entamoeba* parasites[13], suggesting that an *Entamoeba* species could be a candidate host of redondovirus replication as well.

Redondovirus DNA sequences are highly represented in sequencing data from samples of the gingival crevice of periodontitis patients[1,9] and the amoeba *E. gingivalis* contributes the second most abundant ribosomal RNA (rRNA) detected in such samples, after human[14]. Thus *E. gingivalis* is a candidate for the cell hosting redondovirus replication.

The GC content (% GC) of DNA viruses, including CRESS viruses, often mimics that of their hosts[13,15]. We compared the GC content of CRESS virus lineages against those of known or proposed hosts using linear regression (Figure 1B; Table S2). This analysis confirmed the relationship between virus and host GC content ($R^2 = 0.63$, Pearson's Correlation Test p-value = 5.44e-10). The median GC contents of the two *Redondoviridae*

species, *Vientovirus* and *Brisavirus*, are 34.6% and 33.9%, respectively. The genome of *E. gingivalis* has not been sequenced, thus redondovirus GC content was compared to that of the five *Entamoeba* species with complete publicly available genome sequences (*E. histolytica, E. dispar, E. nuttalli, E. invadens, E. moshkovskii*). Similar to redondovirus genomes, *Entamoeba* sequences are of low GC content, ranging from 24.1 to 30.3% depending on the species. In contrast, the GC content of the human genome is 40.9%[16]. This our analysis of GC content points to *Entamoeba* as a more likely host cell for redondovirus replication than human cells. Based on these findings, we investigated *E. gingivalis* as a candidate host for redondovirus replication.

Redondovirus and *E. gingivalis* co-occur in metagenomic data from subjects with oral disease and healthy controls

We quantified whether redondoviruses and *E. gingivalis* co-occurred over a variety of human-derived sample types, as would be expected if *E. gingivalis* is the host cell for redondovirus replication. We queried 58 metagenomic datasets encompassing 7,869 samples from diverse human body sites and disease states for the presence of redondovirus sequences, and then assessed the presence of *E. gingivalis* DNA (Table S3). For this, 81 complete redondovirus genomes and 28 *E. gingivalis* small subunit 18S rRNA genes were used as alignment targets (Table S4; because the genome of *E. gingivalis* has not been fully sequenced, we used the 18S rRNA gene in our queries). Four datasets (NCBI BioProject IDs: PRJEB42701[17], PRJNA552294[18], PRJNA508385[18], PRJNA547717[19]) were positive for redondovirus DNA. The studies all described metagenomic analysis of samples from the oral cavity of healthy individuals and patients with peri-implantitis, mucositis, or periodontitis.

In metagenomic sequence studies of submucosal and subgingival plaque of healthy controls and patients with peri-implantitis or mucositis[19], a distribution was seen of samples that were positive and negative for both *E. gingivalis* and redondovirus sequences, allowing statistical analysis of co-occurrence. In each case, redondoviruses occurrence was found to be highly correlated with that of *E. gingivalis* (Table 1, top three rows).

For samples from periodontitis patients, two datasets were positive for redondovirus DNA and analyzed further[17,18]. *E. gingivalis* was detected in all samples in both datasets, precluding analysis of co-occurrence. We instead compared the maximum coverage of a redondovirus genome to the maximum coverage of an *E. gingivalis* 18S rRNA gene (Figure 2), revealing a strong positive association ($R^2 = 0.493$, Pearson's Correlation Test p-value = 2.501e-9, n = 130).

Redondovirus and *E. gingivalis* co-occur in critically ill patients, COVID-19 patients, and healthy controls when analyzed by quantitative PCR

We next investigated co-occurrence of redondovirus and *E. gingivalis* DNA in disease states previously found to be associated with elevated redondovirus prevalence using quantitative PCR (qPCR) (Table 1, bottom three rows). The PCR amplicons targeted the *E. gingivalis* 18S rRNA gene and a conserved region of the redondovirus *Cap* ORF.

Previously we reported that redondovirus levels were increased in upper respiratory samples from hospitalized patients with acute illness[1]. Here we surveyed oropharyngeal, nasopharyngeal, and endotracheal aspirate samples from 38 medical intensive care unit patients (Table S5). Where multiple samples were available per subject, if any one sample was positive for redondoviruses or *E. gingivalis*, we scored the patient as positive. Of the 38 patients, three were positive for redondoviruses, all of which were also positive for *E. gingivalis* (Table 1, row 4; Fisher's Exact Test p-value = 0.00012).

We also revisited a cohort of 88 subjects hospitalized with COVID-19, where we previously reported an association between redondoviruses and disease severity (Table S5)[8]. Quantification of *E. gingivalis* prevalence showed a positive association between redondoviruses and *E. gingivalis* (Table 1, row 5; Fisher's Exact Test p-value = 3.3e-8).

Lastly, we compared redondovirus and *E. gingivalis* prevalence in human saliva samples from 50 healthy volunteers in Philadelphia (Table S6). These samples were previously characterized for redondovirus prevalence[5]. Here we tested the samples for the presence of *E. gingivalis* DNA. Of the 16 samples that were positive for redondovirus DNA, 15 were also positive for *E. gingivalis* DNA, again showing co-occurrence (Table 1, row 6; Fisher's Exact Test p-value = 9.85e-7).

Redondovirus and *E. gingivalis* co-occur in metatranscriptomic data derived from periodontitis patients

We reasoned that the cells hosting redondovirus replication should contain redondovirus RNA, and thus queried 18 publicly available RNA-seq datasets encompassing 1,879 samples from diverse human body sites (Table S7). We first screened for redondovirus sequences and then asked whether *E. gingivalis* sequences were detectable in the redondovirus-positive datasets. The alignment targets were those described above (Table S4). Two datasets [20,21], both of which contained samples from the gingival crevice of periodontitis patients, were positive for redondovirus RNA and were analyzed further.

The first study sequenced the metatranscriptome of matched healthy and diseased gingiva from three individuals with aggressive periodontitis[20]. All six samples (from both diseased and healthy sites) were positive for *E. gingivalis* RNA. Only the three samples from diseased sites were also positive for redondovirus RNA (Figure 3A–C). Substantially more RNA reads mapped to the *E. gingivalis* alignment targets in the diseased, redondovirus-positive samples (3,486.58 reads per kilobase per million (RPKM)) compared to the healthy, redondovirus-negative samples (33.25 RPKM).

The second study analyzed the metatranscriptome of pooled gingival tissues from periodontitis patients and healthy controls[21]. Both the healthy and diseased pools were positive for *E. gingivalis* RNA, while redondovirus RNA was only detected in the diseased pool (Figure 3D). As before, more RNA reads mapped to the *E. gingivalis* 18S rRNA gene in the diseased, redondovirus-positive sample than in the healthy, redondovirus-negative sample (19.46 RPKM and 11.14 RPKM, respectively).

We then assessed the correlation between the maximum coverage to a redondovirus genome and an *E. gingivalis* 18S rRNA gene across both sequencing studies, which revealed a trend toward positive association ($R^2 = 0.57$, Pearson's Correlation Test p-value = 0.137; not shown).

Detection of redondovirus nucleic acids in a xenic *E. gingivalis* culture

E. gingivalis has not yet been grown in pure culture but can be grown in the presence of feeder bacteria. Such a xenic culture was obtained from ATCC and analyzed (*E. gingivalis* ATCC-30956). The culture contained cells with the morphology expected for *Entamoeba* trophozoites (Figure 4A) and the presence of *E. gingivalis* RNA and DNA was confirmed by qPCR (Figure 4B). The culture was also robustly positive for redondovirus nucleic acids, with 2.06e8 DNA copies/mL and 530.17 RNA copies/mL of culture fluid (Figure 4B). Quantitative PCR analysis targeting human GAPDH yielded no detectable signal, confirming the absence of human cells in the xenic culture. This finding implies that redondoviruses replicate in one of the unicellular organisms present in the xenic culture and not in human cells.

A complete redondovirus genome was recovered from the xenic culture by PCR and DNA sequencing (Figure 4C–E). This genome, named RV-30956, is 3,162 bp in length and encodes the expected Cap, Rep, and ORF3 proteins. To compare redondovirus RV-30956 to previously determined redondovirus sequences, we integrated the RV-30956 Rep sequence into a maximum-likelihood tree of 36 reported redondovirus Rep sequences. This indicated that the redondovirus isolate from the xenic culture is a member of the *Vientovirus* species (Figure 4E). RV-30956 is close in sequence to redondoviruses that have been identified in other human specimens. For instance, RV-30956 Rep and its nearest relative, KY328746.1 Rep, which was isolated from a human respiratory specimen[7], share 71.4% amino acid identity (Figure S1B).

Analysis of the redondovirus host using Hi-C

The detection of redondoviruses in a xenic *E. gingivalis* culture suggests that redondoviruses are capable of replication in the absence of human cells. However, given that the xenic culture was a mixture of cell types, it does not definitively establish *E. gingivalis* as the host cell. Metagenomic analysis showed that overall, the xenic culture was dominated by bacteria (Figure 4F). *E. gingivalis* ribosomal rRNA gene sequences were detectable (96.1% coverage), but not human rRNA gene sequences. Theoretically, one of the bacteria in the xenic culture might serve as the host for redondovirus replication, though as mentioned above, the lack of Shine-Dalgarno sequences in the redondovirus genome and absence of redondovirus sequences among bacterial CRISPR spacers argue against a bacterial host.

To investigate the identity the redondovirus host cell, we performed *in situ* DNA cross-linking using Hi-C[22]. Cells from the xenic *E. gingivalis* culture were partially permeabilized and then exposed to a DNA cross-linking agent to physically link DNA sequences in close proximity, such as redondovirus DNA and genomic DNA from the same cell. By this means, extrachromosomal DNA such as viral replication intermediates can be cross-linked to cellular genomic DNA. Following DNA cleavage and ligation, linked DNA fragments

formed chimeric molecules that can be analyzed by paired-end sequencing, permitting the recovery of chimeric sequences containing extrachromosomal DNA (e.g., the redondovirus genome) linked to the host cell chromosome (Figure 5A). Although CRESS viruses are inferred to package single-stranded DNA in viral particles, replication inside host cells is thought to involve a double-stranded DNA intermediate[23,24].

A total of 114 Hi-C sequence reads matched redondoviruses and had mates that could be identified via BLASTn against the NCBI nucleotide database (Figure 5B). Of those, 101 were linked to mate pairs that also corresponded to redondovirus sequences. In 6 cases, redondovirus reads were paired with reads annotated as *Entamoeba* (Table S8), significantly more than would be expected by chance (in 10,000 random draws, only 10 contained one *E. gingivalis* read, none had more; Permutation test p-value <0.00001). Two reads were identified as linking to bacteria in the genus *Parabacteroides*. No other taxa were identified with more than one read linked to a redondovirus sequence and no reads were found linking redondovirus DNA to human DNA. The degree of enrichment of redondovirus-*Entamoeba* and redondovirus-redondovirus pairs is quantified in Figure 5C. Reads linking redondovirus sequences to bacteria may either arise due to artifactual ligation during sequence library preparation or possibly reflect the presence of bacterial DNA inside *E. gingivalis* cells associated with predation[25]. As a positive control for the Hi-C data, reads aligning to abundant bacterial species were analyzed and shown to be enriched in mate pairs aligning to the same bacterial species (Figure S2). These findings support *E. gingivalis* as a host for redondovirus replication.

DISCUSSION

Sequence analysis of viral particles isolated from human samples commonly yields a majority of reads that do not closely match any known viruses — the virome “dark matter.” Extensive efforts are under way to understand the origin and nature of the full human virome[26–29]. Here we present evidence that a newly annotated family of human-associated viruses, *Redondoviridae*, in fact appear to replicate in the human-associated amoeba *Entamoeba gingivalis*.

While considerable attention has focused on human virome constituents that infect the bacterial microbiome (i.e., bacteriophages), viruses of human eukaryotic commensals remain understudied. Viruses are known that infect a few eukaryotic parasites of humans, including *Leishmania, Giardia, Trichomonas, Cryptosporidium, Plasmodium,* and *Entamoeba*[13,30–40]. In rare cases these viruses have been detected in metagenomic samples from humans. For instance, the CRESS virus family *Naryaviridae* has been proposed to infect *Entamoeba* species and its members have been detected in human stool samples[13]. One of the viral endosymbionts of *Leishmania*, Leishmania RNA virus-1, is reported to enhance *Leishmania* virulence by promoting parasite persistence in the host[41]; it is unknown whether redondovirus infection influences *E. gingivalis* pathogenesis. Given the widespread distribution and high prevalence of redondoviruses in some surveys[1,5–7], these findings underscore that, like viruses of the bacterial microbiome, viruses of human-associated eukaryotic commensals are potentially significant contributors to the human virome. This

work further establishes that a virus of the human oro-respiratory tract can be traced to a eukaryotic commensal host.

Redondoviruses have been previously associated with several human disease states, such as periodontitis, critical illness, and COVID-19[1,8,9]. These earlier observations suggested possible roles for redondoviruses in pathogenesis, but results reported here suggest that redondoviruses may instead be markers for *E. gingivalis* colonization or infection. It is increasingly appreciated that bacteriophages can have direct effects on human cells despite those cells not serving as hosts for infection and are even targets of immune recognition [42–44]; it remains unclear whether redondoviruses have analogous direct effects on human cells.

Studies of periodontitis have previously reported an association of *E. gingivalis* with disease[14,45–48] and results presented here based on tracking with redondovirus DNA raise the question of possible participation in additional disorders. *E. gingivalis* is a common inhabitant of the human oral cavity[14,45–48] and has been detected, though infrequently, in the lungs[49]. Redondoviruses similarly have been commonly found in the oral cavity[1,5,9] and respiratory tract [1,6,8]. While it is possible that *E. gingivalis* may have a broader habitat in humans than has been recognized, it is also plausible that both *E. gingivalis* and redondoviruses translocate from the oral cavity to the lung during disease. Increased detection of redondoviruses and *E. gingivalis* in upper respiratory specimens in some conditions could also result from treatments that affect oral and oropharyngeal drainage, such as endotracheal intubation or alterations in oral hygiene in severe illness. Nevertheless, the importance of *E. gingivalis* colonization and infection in this setting is uninvestigated. Possibilities range from *E. gingivalis* being a benign transient or nonpathogenic colonizer of the respiratory tract to it being a contributor to pathogenesis and/or inflammation. *E. gingivalis* has been documented to ingest human cells[48,50], and *E. gingivalis* can kill live epithelial cells by trogocytosis[51], suggesting pathogenic potential. Our qPCR analysis supported an association of *E. gingivalis* and endotracheal intubation in COVID-19. Thus, it will be useful to investigate the importance of *E. gingivalis* in acute lung injury and respiratory failure more fully.

This study has several limitations. *E. gingivalis* has not been grown in pure culture, thus it was not possible to study redondovirus growth with experimental infections. The inability to grow *E. gingivalis* axenically has also hindered efforts to sequence the parasite genome, which considerably complicated our Hi-C analysis — despite this, we were able to find sufficient numbers of redondovirus sequences linked to recognizable *Entamoeba* sequences to make the association unlikely to be a result of chance. Within our study, difficulties working with the xenic *E. gingivalis* culture precluded further investigation such as fluorescence *in situ* hybridization to colocalize redondovirus and *E. gingivalis* sequences. So far, we have evidence for growth of redondoviruses in cells of *E. gingivalis* only, but our data do not rule out the possibility that redondoviruses may infect additional *Entamoeba* species or other hosts.

In summary, this study provides evidence that the widely prevalent, human-associated redondoviruses replicate in *E. gingivalis* cells. Most studies of the human virome report

abundant viruses replicating in human-associated bacteria, but not viruses of eukaryotic commensals — thus our data focus attention on a little studied part of the human virome. Here we emphasize that human-associated eukaryotes can also contribute commonly encountered members of the human virome. These eukaryotic commensal viruses, in turn, can then be markers for the presence of their hosts, allowing investigation of virus/commensal/human interactions and microbe-disease associations, and may even allow for viral modulation of the eukaryotic microbiome in a manner analogous to phage therapy.

Note added in proof

While this work was under review Kinsella et al. reported based on bioinformatics analysis of published data that presence of redondoviruses correlated with presence of *E. gingivalis* [52].

STAR methods

RESOURCE AVAILABILITY

Lead contacts—Further information and requests for resources and reagents should be directed to and will be fulfilled by the Lead Contact, Frederic Bushman (bushman@pennmedicine.upenn.edu).

Materials availability—This study did not generate any unique reagents.

Data and code availability

- The metatranscriptomic and metagenomic screens used publicly available datasets (NCBI BioProject accessions are listed in Table S3 and Table S7, respectively). The redondovirus sequence obtained from the xenic *E. gingivalis* culture (RV-30956) has been deposited in GenBank under the accession ON986208. Metagenomic and Hi-C raw reads have been deposited in NCBI under the BioProject accession PRJNA858476.
- This study does not report original code and all computational resources used are publicly available as of the date of publication and are listed in the key resources table.
- Any additional information required to reanalyze the data reported in this paper is available from the Lead Contact upon request.

EXPERIMENTAL MODEL AND SUBJECT DETAILS

Human studies—Saliva samples were collected as previously described in [5] from healthy volunteers in Philadelphia following written informed consent under protocol #842613 approved by the institutional IRB. Endotracheal aspirate samples, oropharyngeal swab samples, and nasopharyngeal swabs were collected as previously described in [8] from patients in the medical intensive care unit of the Hospital of the University of Pennsylvania following written or verbal informed consent from patients or surrogates under protocol #823392 approved by the institutional IRB. Specimens were stored at −80°C until processing. Clinical data were extracted from the electronic medical record.

***E. gingivalis* xenic culture conditions—**TYGM-9 medium (ATCC Medium 1171) was purchased from ATCC or prepared in-house according to the manufacturer's instructions (ATCC). To prepare a rice starch solution (a media component), 0.5 g of rice starch (Sigma-Aldrich) was suspended in 9.5 mL of sterile phosphate buffered saline solution (pH 7.4). Undissolved rice starch was removed through centrifugation (100 × g for 5 min). Sterile TYGM-9 medium and starch solution were stored at 4°C.

Culture of *E. gingivalis* was carried out as instructed by staff at ATCC. A xenic *E. gingivalis* culture (ATCC-30956) was obtained from ATCC and upon arrival incubated at a 15° horizontal slant at 35°C for 3 hr. The tube was then gently inverted and centrifuged at 500 × g for 5 min to pellet *E. gingivalis* cells. To generate bacterized medium, 250 uL of the supernatant (containing bacteria) was removed from the culture and added to another tube containing 10 mL of fresh TYGM-9 medium. All but ~1 mL of the remaining supernatant was divided among eight 16 × 125 mm screw-capped tubes and fresh TYGM-9 medium was added to increase the volume of each tube to 8 mL. The remaining culture material (a cell pellet and ~1 mL of supernatant) was stored on ice for 5 min, inverted 20 times, and transferred as 0.1-mL aliquots to the eight tubes. The ratio of rice starch and bacterized medium was varied among subcultures in an effort to optimize growth. All subcultures, in addition to the tube of bacterized TYGM-9 medium, were incubated a 15° horizontal slant at 35°C. Every 24–48 hr, the procedure described above was repeated on all subcultures.

E. gingivalis culture viability was confirmed every 72 hr using trypan blue staining. After inverting each sub-culture 10 times, a 1-mL aliquot was centrifuged for 500 × g for 5 min, and the cell pellet was resuspended in 100 uL of PBS. 10 uL of 0.4% trypan blue (Sigma-Aldrich) was mixed with 10 uL of the cell suspension. After a 3 min incubation at room temperature, 10 uL of the mixture was deposited on a microscope slide and a coverslip was applied. An inverted binocular microscope was used to view the sample and permit the enumeration of viable (unstained) and non-viable (stained) *E. gingivalis* cells.

To image the xenic *E. gingivalis* culture, 500 uL of culture material was pelleted at 500 × g for 10 min and resuspended in 500 uL of sterile saline. Next 10 uL was deposited onto microscope slides using a Cytopro cytospin (ELITechGroup Inc) (1,000 × g for 5 min). Slides were air-dried, fixed in methanol, and stained using a Kwik Diff staining kit (Methylene blue and eosin) (Fisher Scientific) following the manufacturer's instructions (Epredia) prior to being viewed under a microscope at 40X and 100X magnification (oil immersion lens).

METHOD DETAILS

DNA isolation—DNA was extracted from human specimens (e.g., saliva, oropharyngeal swabs, nasopharyngeal swabs, endotracheal aspirates) using the DNeasy Blood and Tissue Kit (Qiagen). When saliva was used as the starting material, the following modifications to the manufacturer's protocol were made: 250 uL of saliva were used as the starting input in Step 1, 250 uL of ethanol were used in Step 5, and a repeat elution step was performed using the initial eluate to maximize DNA yield. When an aliquot of *E. gingivalis* xenic culture material was used as the starting material, the following modifications to the manufacturer's protocol were made: 200 uL of liquid culture were used as the starting input in Step 1 and

a repeat elution step was performed using the initial eluate to maximize DNA yield. When human peripheral blood mononuclear cells or human 293T cells were used as the starting material, the protocol was followed with no modification. DNA purity was determined using a Nanodrop 2000/200C spectrophotometer (Thermo Fisher) and DNA yield was measured using PicoGreen (Affymetrix) quantification. Isolated DNA was stored at −20°C.

RNA isolation—RNA was extracted using the RNeasy Mini Kit (Qiagen). When an aliquot of *E. gingivalis* culture was used as the starting material, the following modification to the manufacturer's protocol was made: 300 uL of liquid media were used as the starting material and 300 uL of Buffer RLT were used for Step 1. The optional on-column DNase digestion referenced in Step 5 was performed using DNase I Reaction Buffer (10X, 1X final concentration) (New England Biolabs, NEB) and RNase-free H_2O. RNA purity and yield were determined using an Eppendorf BioPhotometer D30 (Eppendorf). Isolated RNA was stored at −80°C.

Multiple displacement amplification and quantitative PCR—For redondovirus detection (presence/absence), extracted DNA was subjected to multiple displacement amplification (MDA), which is sequence-unbiased but preferentially amplifies circular DNA, followed by qPCR; for quantification, extracted DNA was subject to qPCR without prior MDA. MDA and qPCR were performed as previously described[1,59,60].

In brief, MDA was carried out using Phi29 Buffer (10X, 1X final concentration) (NEB), BSA (20 mg/mL, 0.1 mg/mL final concentration) (NEB), Phi29 DNA Polymerase (10 units/uL, 10 units final concentration) (NEB), random hexamers (50 uM, 2 uM final concentration) (Invitrogen), dNTPs (10 mM, 1mM final concentration) (NEB), and molecular grade H_2O. MDA used the following conditions on a Veriti 96-well thermocycler (Thermo Fisher): 35°C for 5 min, 34°C for 10 min, 33°C for 15 min, 32°C for 20 min, 31°C for 30 min, 30°C for 16 h, and a final extension at 65°C for 15 min.

For the detection and quantification of redondovirus DNA, MDA-amplified and unamplified DNA samples were run in duplicate in a real-time qPCR assay using TaqMan Fast Universal Master Mix (2X, 1X final concentration) (Thermo Fisher), primer-probe mix (Integrated DNA Technologies (IDT)) based on conserved segments of the redondovirus genome (F: 5'-GGATGCCATGAAACTTTGATAC-3'; R: 5'-TCTTCCTCCTTATTTGTATGGC-3'; probe: 5'-CCCATACTTACGCCGGTTACCTGC-3'), and molecular grade H_2O. The following conditions were used for the PCR reaction: 50°C for 2 min, 95°C for 10 min; 40 cycles of 95°C for 15 sec and 60°C for 1 min; and a final extension at 4°C.

For the detection and quantification of redondovirus RNA, RNA samples were run in duplicate in a real-time RT-qPCR assay using TaqMan Fast Virus 1-Step Master Mix (4X, 1X final concentration) (Thermo Fisher), primer-probe mix (IDT) targeting the Cap ORF (F: 5'-GGATGCCATGAAACTTTGATAC-3'; R: 5'-TCTTCCTCCTTATTTGTATGGC-3'; probe: 5'-CCCATACTTACGCCGGTTACCTGC-3'), and molecular grade H_2O. Reverse transcription was carried out at 50°C for 5 min. The following conditions were used for the PCR reaction: 95°C for 20 sec; 40 cycles of 95°C for 3 sec and 60°C for 30 sec; and a final extension at 4°C.

For redondovirus qPCR and RT-qPCR, a standard curve was generated from serial dilutions of a plasmid (pUC57) containing the cloned genome of brisavirus AA. qPCRs were run on a QuantStudio5 (Thermo Fisher) machine using the “Fast” mode. Negative controls consistently showed a cycle threshold (CT) of >40 cycles, so positive samples were defined as samples with any CT value <40 cycles. Non-template controls and extraction controls were included in qPCR assays; no negative controls showed amplification. In cases where multiple samples were queried per patient, if one sample was found to be positive for redondoviruses, the patient was scored as positive.

E. gingivalis qPCR was performed as previously described in [47]. For *E. gingivalis* DNA detection, samples were run in duplicate in a real-time qPCR assay using PowerUp SYBR Green Mix (2X, 1X final concentration) (Thermo Fisher), $MgCl_2$ (25 mM, 3 mM final concentration), primer mix (IDT) targeting the 18S rRNA gene (F: 5’-TACCATACAAGGAATAGCTTTGTGAATAA-3’; R: 5’-ACAATTGTAAATTTGTTCTTTTTCT-3’), and molecular grade H_2O. The following conditions were used for the PCR reaction: 50°C for 2 min, 95°C for 2 min; 40 cycles of 95°C for 15 sec, 60°C for 15 sec, 72°C for 1 min; 95°C for 15 sec, 66°C for 1 min, 40°C for 30 sec; and a final extension at 4°C. Isolated RNA was reverse transcribed into cDNA using a SuperScript III First-Strand Synthesis System Kit (Invitrogen). For *E. gingivalis* RNA detection and quantification, the qPCR protocol described above was used with cDNA as the template.

For *E. gingivalis* qPCR, a standard curve made from serial dilutions of a synthetic gene block (IDT) encoding an *E. gingivalis* 18S rRNA gene (NCBI accession: KX027295.1) was included in each run. qPCRs were run on a QuantStudio5 (Thermo Fisher) machine. Negative controls consistently showed a cycle threshold (CT) value of ≥40 cycles, so positive samples were defined as samples with any CT value <40 cycles. Non-template controls and extraction controls were included in qPCR assays. In cases where multiple samples were queried per patient, if one sample was found to be positive for *E. gingivalis*, the patient was scored as positive.

For the detection of human DNA, DNA samples were run in triplicate in a real-time qPCR assay using TaqMan Fast Universal Master Mix (2X, 1X final concentration) (Applied Biosystems), primer-probe mix (IDT) targeting the GAPDH gene (F: 5’-GGTGGTCTCCTCTGACTTCAACA-3’; R: 5’-CCAGCCACATACCAGGAAATG-3’; probe: 5’-CTGGCATTGCCCTCAACGACCAC-3’ [61]), and molecular grade H_2O. The following conditions were used for the PCR reaction: 50°C for 2 min, 95°C for 10 min; 40 cycles of 95°C for 15 sec and 60°C for 1 min; and a final extension at 4°C. Two standard curves were generated from serial dilutions of DNA isolated from human peripheral blood mononuclear cells and human 293T cells. Negative controls consistently showed a CT value of ≥40 cycles, thus positive samples were defined as samples with any CT value <40 cycles.

Redondovirus whole-genome sequencing from the xenic culture

To recover the complete redondovirus genome from the xenic culture, two whole-genome PCRs were performed with nonoverlapping primer sets (Set A F: 5’-CCTTTGGTCTCGAAATCTTCCTATACTGG-3’;

Set A R: 5'-AGGCCTCTCTCCCTTCCATTTGG-3'; Set B F: 5'GGTTATCGTTCATTTGATCATGCATTAGTACC-3'; Set B R: 5'-ACCAAGATGTTTAAGCCCTTTAGTTAATGTTTC-3') using the Phusion PCR Kit (NEB) and the following PCR settings: 98°C for 30 sec, then 35 cycles of 98°C for 10 sec, 55°C for 15 sec, and 72°C for 1 min 30 sec, followed by a final extension of 10 min at 72°C. The ~3-kb PCR products were visualized on a 1% agarose gel, excised, and purified from gels using a Monarch DNA Gel Extraction Kit (NEB). The manufacturer's protocol was used with the modification of a 15-uL H_2O final elution. After gel extraction, libraries were prepared from PCR products using the Nextera XT DNA Library Preparation Kit (Illumina). Libraries were sequenced using the Illumina MiSeq platform (Illumina).

Read processing and genome assembly

Sunbeam (v2.1)[62], a Snakemake-based pipeline[63], was used for quality control, host decontamination, and contig assembly as previously described[1,62]. Trimmomatic (v0.39)[64] and FastQC (v0.11.9) were used for adapter trimming and read quality control, respectively. Contigs were assembled from quality-controlled reads using MEGAHIT (v1.2.9)[65] and annotated using BLAST against a database of published redondovirus genome sequences[1,58]. A Sunbeam extension (sbx_select_contigs, https://github.com/ArwaAbbas/sbx_select_contigs) was used to extract contigs with homology to redondoviruses (as annotated by BLAST). Extracted contigs were overlap-assembled using CAP3 (v3.0)[66], circularized based on the overlaps identified by sbx_select_contigs, and polished by aligning quality-controlled reads to the draft genomes. Visualization of alignments in Integrated Genomics Viewer (IGV) (v2.9.0)[67] permitted the manual correction of assembly errors, which were rare.

Phylogenetic analysis

For the ssDNA virus phylogenetic tree (Figure S1), we used ViPTree (v3.1) to generate a "proteomic tree" of 2,164 viral genome sequences (10 redondovirus genomes and 2,154 genomes of eukaryotic and prokaryotic viruses in the ViPTree ssDNA database; Table S1) based on genome-wide sequence similarities computed by tBLASTx[68]. iTOL (v6) was used for tree visualization and clade collapsing (based on average BRL (>0.4))[55].

For the *Cressdnaviricota* tree (Figure 1A), alignments of CRESS virus Rep sequences were performed using MUSCLE (v3.8.31)[53]. From the alignments, trees were constructed using RAxML (v8.2)[54] and visualized using iTOL (v6)[55].

For the *Redondoviridae* tree (Figure 4E), redondovirus Rep amino acid sequences were aligned using MUSCLE (v3.8.31)[53]. Phylogenetic trees were constructed from sequence alignments using PhyML (v3.0)[56] and visualized using iTOL (v6)[55].

Hi-C and shotgun library generation and sequencing

A chromatin interaction (Hi-C) library was generated using the Proximo Hi-C (Microbe) Kit (Phase Genomics). After starting with DNA from 200 uL of *E. gingivalis* culture material, the ProxiMeta Hi-C protocol (v4.0) was followed without modification using proprietary materials supplied with the kit. Cells were partially permeabilized and exposed to a DNA

crosslinker. Cells were lysed to release the crosslinked DNA into the supernatant and enable DNA recovery by centrifugation. Endonucleases were then used to fragment the crosslinked DNA. Fragmented DNAs were biotinylated and ligated to create chimeric junctions between adjacent sequences (i.e., sequences that originated from the same cell). Crosslinks were then reversed and the DNA was purified using a streptavidin bead pull down. Streptavidin-bound DNA was quantified using Qubit dsDNA HS, which was used to determine the subsequent adapter dilution and number of PCR cycles. Next a Hi-C library was prepared and on-bead amplification was performed using the Nextera XT DNA Library Preparation Kit (Illumina). In addition, a standard shotgun library of total DNA isolated from the *E. gingivalis* culture was prepared using the Nextera XT DNA Library Preparation Kit (Illumina) and sequenced to compare to the Hi-C library. Both were sequenced using the Illumina NextSeq 500 platform (Illumina), generating 150 bp paired-end reads. Proximity-ligated reads were mapped against shotgun sequencing data to inform in-cell DNA interactions. 29,415,700 and 109,616,621 reads were obtained from sequencing the shotgun and Hi-C libraries, respectively.

QUANTIFICATION AND STATISTICAL ANALYSIS

Querying public sequence data for redondovirus and *E. gingivalis* DNA and RNA—To investigate the presence of redondovirus DNA, we queried 58 metagenomic datasets (Table S3). 81 redondovirus virus genomes and 28 *E. gingivalis* 18S rRNA genes downloaded from GenBank (NCBI) were used as local alignment targets (Table S4)[69,70]. Alignments were performed using the hisss pipeline (https://github.com/louiejtaylor/hisss) [1], which uses Bowtie 2 (option, –very-sensitive-local)[71] to align reads to target genomes, SAMtools[72] and BEDtools[73] to calculate the coverage of the reads to the target genomes, and ggplot2 in R (v3.3.6) to visualize the alignments. Positive identification was defined as ≥5% coverage to any redondovirus genome or 18S rRNA gene sequence.

To investigate the presence of redondovirus RNA, we queried 18 metatranscriptomic datasets (Table S7) for redondovirus and *E. gingivalis* RNA (Table S4). The hisss pipeline was used as described above to perform alignments, calculate read coverage to target sequences, and visualize alignments. Positive identification was prospectively defined as ≥0.05 fractional coverage (≥5% coverage) to a redondovirus genome or an *E. gingivalis* 18S rRNA gene.

Analysis of xenic culture metagenome—Taxonomic assignment of the quality-controlled reads was performed with Kraken2 (v2.1.2)[57] using the Standard database (archaea, bacteria, viral, plasmid, human, UniVec_Core) and the PlusPF database (standard database plus protozoa and fungi) (https://benlangmead.github.io/aws-indexes/k2). To supplement the Kraken2 results and capture low-abundance taxa of interest (*Redondoviridae, Entamoeba*), we performed BLASTn on 10 million reads before estimating relative abundance[58].

We used 18S rRNA genes belonging to *E. gingivalis* and *Homo sapiens* to query of the metagenomic data obtained from the *E. gingivalis* culture. The hisss pipeline was used

as described above to align the sequencing reads to the alignment targets and calculate coverage of the target sequences.

Hi-C analysis—To assess whether redondovirus genomes resided in the same cells as the *E. gingivalis* genome, we assessed Hi-C crosslinking between redondovirus and *Entamoeba* sequences. We created a custom BLASTn database of all available redondovirus genomes from the NCBI nt database[58]. All Hi-C reads were aligned to this database, identifying 246 forward or reverse reads classified as *Redondoviridae*. The read mate pairs for each *Redondoviridae* read were then aligned via BLASTn to the complete nt database (downloaded January 2022). Because there is no whole genome sequence available for *Entamoeba gingivalis*, we accepted alignments to any member of the *Entamoeba* genus. We identified 6 chimeric reads indicative of *Entamoeba*-redondovirus cross-linking (Figure 5; Table S8). To determine the probability of 6 reads aligning to *Entamoeba* by chance in our data, we took 100,000 random draws of 246 reads and counted *Entamoeba* reads using the same BLASTn search. As a positive control, reads were identified matching the most abundant bacterial genera in the xenic culture, and mate pairs verified to be highly enriched in sequences aligning to the same bacterial genus (Figure S2). Alignments were carried out using BLAST querying the NCBI database.

Statistical tests—Co-occurrence of redondoviruses and *E. gingivalis* was assessed using Fisher's Exact Test (Table 1). Association of virus and host GC content was assessed using Pearson's Correlation Test (Figure 1). Association of redondovirus and *E. gingivalis* relative abundance was assessed using Pearson's Correlation Test (Figure 2). The probability of identifying Hi-C mate pairs by chance was calculated by a permutation test based on 100,000 random draws of 246 reads and counting *Entamoeba* reads using a BLASTn search.

Supplementary Material

Refer to Web version on PubMed Central for supplementary material.

ACKNOWLEDGEMENTS

We are grateful to the individuals who provided samples for analysis. We thank members of the Bushman and Collman labs for helpful discussions and suggestions, Laurie Zimmerman and Arwa Abbas for help with illustrations, and staff at ATCC for guidance on management of the *E. gingivalis* xenic culture. This work was supported by NIH grant R33-HL137063 (R.G.C., F.D.B.); the PennCHOP Microbiome Program; and NIH grant R35 GM134957-01; National Institute of Allergy and Infectious Diseases, National Institutes of Health, Department of Health and Human Services, under Contract No. 75N93021C00015 (CEIRR); and American Diabetes Association Pathway to Stop Diabetes grant #1-19-VSN-02 (ST). We acknowledge assistance from multiple cores of the Penn Center for AIDS Research (P30-AI45008) and the Penn Center for Research on Coronaviruses and Other Emerging Pathogens.

REFERENCES

1. Abbas AA, Taylor LJ, Dothard MI, Leiby JS, Fitzgerald AS, Khatib LA, Collman RG, and Bushman FD (2019). Redondoviridae, a Family of Small, Circular DNA Viruses of the Human Oro-Respiratory Tract Associated with Periodontitis and Critical Illness. Cell Host Microbe 26, 297. 10.1016/j.chom.2019.07.015. [PubMed: 31415757]
2. Cui L, Wu B, Zhu X, Guo X, Ge Y, Zhao K, Qi X, Shi Z, Zhu F, Sun L, and Zhou M.(2017). Identification and genetic characterization of a novel circular single-stranded DNA virus in a human

upper respiratory tract sample. Arch Virol 162, 3305–3312. 10.1007/s00705-017-3481-3. [PubMed: 28707271]

3. Krupovic M, Varsani A, Kazlauskas D, Breitbart M, Delwart E, Rosario K, Yutin N, Wolf YI, Harrach B, Zerbini FM, et al. (2020). Cressdnaviricota: a Virus Phylum Unifying Seven Families of Rep-Encoding Viruses with Single-Stranded, Circular DNA Genomes. J Virol 94. 10.1128/JVI.00582-20.
4. Abbas A, Taylor LJ, Collman RG, Bushman FD, and Ictv Report C.(2021). ICTV Virus Taxonomy Profile: Redondoviridae. J Gen Virol 102. 10.1099/jgv.0.001526.
5. Taylor LJ., Dothard MI., Rubel MA., Allen AA., Hwang Y., Roche AM., Graham-Wooten J., Fitzgerald AS., Khatib LA., Ranciaro A., et al. . (2021). Redondovirus Diversity and Evolution on Global, Individual, and Molecular Scales. J Virol 95, e0081721. 10.1128/JVI.00817-21. [PubMed: 34406857]
6. Spezia PG, Macera L, Mazzetti P, Curcio M, Biagini C, Sciandra I, Turriziani O, Lai M, Antonelli G, Pistello M, and Maggi F.(2020). Redondovirus DNA in human respiratory samples. J Clin Virol 131, 104586. 10.1016/j.jcv.2020.104586. [PubMed: 32841923]
7. Lazaro-Perona F, Dahdouh E, Roman-Soto S, Jimenez-Rodriguez S, Rodriguez-Antolin C, de la Calle F, Agrifoglio A, Membrillo FJ, Garcia-Rodriguez J, and Mingorance J.(2020). Metagenomic Detection of Two Vientoviruses in a Human Sputum Sample. Viruses 12. 10.3390/v12030327.
8. Merenstein C, Liang G, Whiteside SA, Cobian-Guemes AG, Merlino MS, Taylor LJ, Glascock A, Bittinger K, Tanes C, Graham-Wooten J, et al. (2021). Signatures of COVID-19 Severity and Immune Response in the Respiratory Tract Microbiome. mBio 12, e0177721. 10.1128/mBio.01777-21. [PubMed: 34399607]
9. Zhang Y, Wang C, Feng X, Chen X, and Zhang W.(2021). Redondoviridae and periodontitis: a case-control study and identification of five novel redondoviruses from periodontal tissues. Virus Evol 7, veab033. 10.1093/ve/veab033. [PubMed: 35186324]
10. Krishnamurthy SR, and Wang D.(2018). Extensive conservation of prokaryotic ribosomal binding sites in known and novel picobirnaviruses. Virology 516, 108–114. 10.1016/j.virol.2018.01.006. [PubMed: 29346073]
11. Gophna U, and Brodt A.(2012). CRISPR/Cas systems in archaea: What array spacers can teach us about parasitism and gene exchange in the 3rd domain of life. Mob Genet Elements 2, 63–64. 10.4161/mge.19907. [PubMed: 22754756]
12. Barrangou R., Fremaux C., Deveau H., Richards M., Boyaval P., Moineau S., Romero DA., and Horvath P. (2007). CRISPR provides acquired resistance against viruses in prokaryotes. Science 315, 1709–1712. 10.1126/science.1138140. [PubMed: 17379808]
13. Kinsella CM, Bart A, Deijs M, Broekhuizen P, Kaczorowska J, Jebbink MF, van Gool T, Cotten M, and van der Hoek L.(2020). Entamoeba and Giardia parasites implicated as hosts of CRESS viruses. Nat Commun 11, 4620. 10.1038/s41467-020-18474-w. [PubMed: 32934242]
14. Deng ZL, Szafranski SP, Jarek M, Bhuju S, and Wagner-Dobler I.(2017). Dysbiosis in chronic periodontitis: Key microbial players and interactions with the human host. Sci Rep 7, 3703. 10.1038/s41598-017-03804-8. [PubMed: 28623321]
15. Cardinale DJ, and Duffy S.(2011). Single-stranded genomic architecture constrains optimal codon usage. Bacteriophage 1, 219–224. 10.4161/bact.1.4.18496. [PubMed: 22334868]
16. Piovesan A, Pelleri MC, Antonaros F, Strippoli P, Caracausi M, and Vitale L.(2019). On the length, weight and GC content of the human genome. BMC Res Notes 12, 106. 10.1186/s13104-019-4137-z. [PubMed: 30813969]
17. Plachokova AS, Andreu-Sanchez S, Noz MP, Fu J, and Riksen NP (2021). Oral Microbiome in Relation to Periodontitis Severity and Systemic Inflammation. Int J Mol Sci 22. 10.3390/ijms22115876.
18. Altabtbaei K., Maney P., Ganesan SM., Dabdoub SM., Nagaraja HN., and Kumar PS. (2021). Anna Karenina and the subgingival microbiome associated with periodontitis. Microbiome 9, 97. 10.1186/s40168-021-01056-3. [PubMed: 33941275]
19. Ghensi P, Manghi P, Zolfo M, Armanini F, Pasolli E, Bolzan M, Bertelle A, Dell'Acqua F, Dellasega E, Waldner R, et al. (2020). Strong oral plaque microbiome signatures for dental implant

diseases identified by strain-resolution metagenomics. NPJ Biofilms Microbiomes 6, 47. 10.1038/s41522-020-00155-7. [PubMed: 33127901]

20. Jorth P, Turner KH, Gumus P, Nizam N, Buduneli N, and Whiteley M.(2014). Metatranscriptomics of the human oral microbiome during health and disease. mBio 5, e01012–01014. 10.1128/mBio.01012-14. [PubMed: 24692635]
21. Kim YG, Kim M, Kang JH, Kim HJ, Park JW, Lee JM, Suh JY, Kim JY, Lee JH, and Lee Y. (2016). Transcriptome sequencing of gingival biopsies from chronic periodontitis patients reveals novel gene expression and splicing patterns. Hum Genomics 10, 28. 10.1186/s40246016-0084-0. [PubMed: 27531006]
22. van Berkum NL, Lieberman-Aiden E, Williams L, Imakaev M, Gnirke A, Mirny LA, Dekker J, and Lander ES (2010). Hi-C: a method to study the three-dimensional architecture of genomes. J Vis Exp. 10.3791/1869.
23. Taylor LJ, Keeler EL, Bushman FD, and Collman RG (2022). The enigmatic roles of Anelloviridae and Redondoviridae in humans. Curr Opin Virol 55, 101248. 10.1016/j.coviro.2022.101248. [PubMed: 35870315]
24. Zhao L, Rosario K, Breitbart M, and Duffy S.(2019). Eukaryotic Circular Rep-Encoding Single-Stranded DNA (CRESS DNA) Viruses: Ubiquitous Viruses With Small Genomes and a Diverse Host Range. Adv Virus Res 103, 71–133. 10.1016/bs.aivir.2018.10.001. [PubMed: 30635078]
25. Garcia LS (2001). Diagnostic Medical Parasitology, 4th ed. Edition (ASM Press).
26. Liang G, and Bushman FD (2021). The human virome: assembly, composition and host interactions. Nat Rev Microbiol 19, 514–527. 10.1038/s41579-021-00536-5. [PubMed: 33785903]
27. Kumata R, Ito J, Takahashi K, Suzuki T, and Sato K.(2020). A tissue level atlas of the healthy human virome. BMC Biol 18, 55. 10.1186/s12915-020-00785-5. [PubMed: 32493363]
28. Tisza MJ, and Buck CB (2021). A catalog of tens of thousands of viruses from human metagenomes reveals hidden associations with chronic diseases. Proc Natl Acad Sci U S A 118. 10.1073/pnas.2023202118.
29. Krishnamurthy SR, and Wang D.(2017). Origins and challenges of viral dark matter. Virus Res 239, 136–142. 10.1016/j.virusres.2017.02.002. [PubMed: 28192164]
30. Widmer G, Comeau AM, Furlong DB, Wirth DF, and Patterson JL (1989). Characterization of a RNA virus from the parasite Leishmania. Proc Natl Acad Sci U S A 86, 5979–5982. 10.1073/pnas.86.15.5979. [PubMed: 2762308]
31. Cantanhede LM., Fernandes FG., Ferreira GEM., Porrozzi R., Ferreira RGM., and Cupolillo E. (2018). New insights into the genetic diversity of Leishmania RNA Virus 1 and its species-specific relationship with Leishmania parasites. PLoS One 13, e0198727. 10.1371/journal.pone.0198727. [PubMed: 29912912]
32. Scheffter SM, Ro YT, Chung IK, and Patterson JL (1995). The complete sequence of Leishmania RNA virus LRV2–1, a virus of an Old World parasite strain. Virology 212, 84–90. 10.1006/viro.1995.1456. [PubMed: 7676652]
33. Nalcaci M, Karakus M, Yilmaz B, Demir S, Ozbilgin A, Ozbel Y, and Toz S.(2019). Detection of Leishmania RNA virus 2 in Leishmania species from Turkey. Trans R Soc Trop Med Hyg 113, 410–417. 10.1093/trstmh/trz023. [PubMed: 31034027]
34. Grybchuk D, Macedo DH, Kleschenko Y, Kraeva N, Lukashev AN, Bates PA, Kulich P, Lestinova T, Volf P, Kostygov AY, and Yurchenko V.(2020). The First Non-LRV RNA Virus in Leishmania. Viruses 12. 10.3390/v12020168.
35. Wang AL, and Wang CC (1986). Discovery of a specific double-stranded RNA virus in Giardia lamblia. Mol Biochem Parasitol 21, 269–276. 10.1016/0166-6851(86)90132-5. [PubMed: 3807947]
36. Goodman RP, Ghabrial SA, Fichorova RN, and Nibert ML (2011). Trichomonasvirus: a new genus of protozoan viruses in the family Totiviridae. Arch Virol 156, 171–179. 10.1007/s00705-010-0832-8. [PubMed: 20976609]
37. Goodman RP., Freret TS., Kul T., Geller AM., Talkington MW., Tang-Fernandez V., Suciu O., Demidenko AA., Ghabrial SA., Beach DH., et al. . (2011). Clinical isolates of Trichomonas vaginalis concurrently infected by strains of up to four Trichomonasvirus species (Family Totiviridae). J Virol 85, 4258–4270. 10.1128/JVI.00220-11. [PubMed: 21345965]

38. Khramtsov NV, Woods KM, Nesterenko MV, Dykstra CC, and Upton SJ (1997). Virus-like, double-stranded RNAs in the parasitic protozoan Cryptosporidium parvum. Mol Microbiol 26, 289–300. 10.1046/j.1365-2958.1997.5721933.x. [PubMed: 9383154]
39. Nibert ML, Woods KM, Upton SJ, and Ghabrial SA (2009). Cryspovirus: a new genus of protozoan viruses in the family Partitiviridae. Arch Virol 154, 1959–1965. 10.1007/s00705-009-0513-7. [PubMed: 19856142]
40. Charon J, Grigg MJ, Eden JS, Piera KA, Rana H, William T, Rose K, Davenport MP, Anstey NM, and Holmes EC (2019). Novel RNA viruses associated with Plasmodium vivax in human malaria and Leucocytozoon parasites in avian disease. PLoS Pathog 15, e1008216. 10.1371/journal.ppat.1008216. [PubMed: 31887217]
41. Ives A, Ronet C, Prevel F, Ruzzante G, Fuertes-Marraco S, Schutz F, Zangger H, Revaz-Breton M, Lye LF, Hickerson SM, et al. (2011). Leishmania RNA virus controls the severity of mucocutaneous leishmaniasis. Science 331, 775–778. 10.1126/science.1199326. [PubMed: 21311023]
42. Sweere JM, Van Belleghem JD, Ishak H, Bach MS, Popescu M, Sunkari V., Kaber G., Manasherob R., Suh GA., Cao X., et al. . (2019). Bacteriophage trigger antiviral immunity and prevent clearance of bacterial infection. Science 363. 10.1126/science.aat9691.
43. Gogokhia L, Buhrke K, Bell R, Hoffman B, Brown DG, Hanke-Gogokhia C, Ajami NJ, Wong MC, Ghazaryan A, Valentine JF, et al. (2019). Expansion of Bacteriophages Is Linked to Aggravated Intestinal Inflammation and Colitis. Cell Host Microbe 25, 285–299 e288. 10.1016/j.chom.2019.01.008. [PubMed: 30763538]
44. Popescu M, Van Belleghem JD, Khosravi A, and Bollyky PL (2021). Bacteriophages and the Immune System. Annu Rev Virol 8, 415–435. 10.1146/annurev-virology-091919-074551. [PubMed: 34014761]
45. Yaseen A, Mahafzah A, Dababseh D, Taim D, Hamdan AA, Al-Fraihat E, Hassona Y, Sahin GO, Santi-Rocca J, and Sallam M.(2021). Oral Colonization by Entamoeba gingivalis and Trichomonas tenax: A PCR-Based Study in Health, Gingivitis, and Periodontitis. Front Cell Infect Microbiol 11, 782805. 10.3389/fcimb.2021.782805. [PubMed: 34950608]
46. Kikuta N, Yamamoto A, and Goto N.(1996). Detection and identification of Entamoeba gingivalis by specific amplification of rRNA gene. Can J Microbiol 42, 1248–1251. 10.1139/m96-161. [PubMed: 8989863]
47. Trim RD, Skinner MA, Farone MB, Dubois JD, and Newsome AL (2011). Use of PCR to detect Entamoeba gingivalis in diseased gingival pockets and demonstrate its absence in healthy gingival sites. Parasitol Res 109, 857–864. 10.1007/s00436-011-2312-9. [PubMed: 21400116]
48. Bonner M., Amard V., Bar-Pinatel C., Charpentier F., Chatard JM., Desmuyck Y., Ihler S., Rochet JP., Roux de La Tribouille V, Saladin L, et al. . (2014). Detection of the amoeba Entamoeba gingivalis in periodontal pockets. Parasite 21, 30. 10.1051/parasite/2014029. [PubMed: 24983705]
49. Jian B, Kolansky AS, Baloach ZW, and Gupta PK (2008). Entamoeba gingivalis pulmonary abscess - diagnosed by fine needle aspiration. Cytojournal 5, 12. 10.4103/1742-6413.43179. [PubMed: 19495399]
50. Bao X, Wiehe R, Dommisch H, and Schaefer AS (2020). Entamoeba gingivalis Causes Oral Inflammation and Tissue Destruction. J Dent Res 99, 561–567. 10.1177/0022034520901738. [PubMed: 32023135]
51. Bao X, Weiner J 3rd, Meckes O, Dommisch H, and Schaefer AS (2021). Entamoeba gingivalis Exerts Severe Pathogenic Effects on the Oral Mucosa. J Dent Res 100, 771–776. 10.1177/00220345211004498. [PubMed: 33792418]
52. Kinsella CM, Deijs M, Becker C, Broekhuizen P, van Gool T, Bart A, Schaefer AS, and van der Hoek L.(2022). Host prediction for disease-associated gastrointestinal cressdnaviruses. Virus Evol 8. 10.1093/ve/veac087.
53. Edgar RC (2004). MUSCLE: multiple sequence alignment with high accuracy and high throughput. Nucleic Acids Res 32, 1792–1797. 10.1093/nar/gkh340. [PubMed: 15034147]
54. Stamatakis A, Ludwig T, and Meier H.(2005). RAxML-III: a fast program for maximum likelihood-based inference of large phylogenetic trees. Bioinformatics 21, 456–463. 10.1093/bioinformatics/bti191. [PubMed: 15608047]

55. Letunic I, and Bork P.(2019). Interactive Tree Of Life (iTOL) v4: recent updates and new developments. Nucleic Acids Res 47, W256–W259. 10.1093/nar/gkz239. [PubMed: 30931475]
56. Guindon S., Lethiec F., Duroux P., and Gascuel O. (2005). PHYML Online--a web server for fast maximum likelihood-based phylogenetic inference. Nucleic Acids Res 33, W557–559. 10.1093/nar/gki352. [PubMed: 15980534]
57. Wood DE, Lu J, and Langmead B.(2019). Improved metagenomic analysis with Kraken 2. Genome Biol 20, 257. 10.1186/s13059-019-1891-0. [PubMed: 31779668]
58. Altschul SF, Gish W, Miller W, Myers EW, and Lipman DJ (1990). Basic local alignment search tool. J Mol Biol 215, 403–410. 10.1016/S0022-2836(05)80360-2. [PubMed: 2231712]
59. Leichty AR, and Brisson D.(2014). Selective whole genome amplification for resequencing target microbial species from complex natural samples. Genetics 198, 473–481. 10.1534/genetics.114.165498. [PubMed: 25096321]
60. Dean FB, Hosono S, Fang L, Wu X, Faruqi AF, Bray-Ward P, Sun Z, Zong Q, Du Y, Du J, et al. (2002). Comprehensive human genome amplification using multiple displacement amplification. Proc Natl Acad Sci U S A 99, 5261–5266. 10.1073/pnas.082089499. [PubMed: 11959976]
61. Yi Y, Shaheen F, and Collman RG (2005). Preferential use of CXCR4 by R5X4 human immunodeficiency virus type 1 isolates for infection of primary lymphocytes. J Virol 79, 1480–1486. 10.1128/JVI.79.3.14801486.2005. [PubMed: 15650174]
62. Clarke EL., Taylor LJ., Zhao C., Connell A., Lee JJ., Fett B., Bushman FD., and Bittinger K. (2019). Sunbeam: an extensible pipeline for analyzing metagenomic sequencing experiments. Microbiome 7, 46. 10.1186/s40168-019-0658-x. [PubMed: 30902113]
63. Koster J, and Rahmann S.(2012). Snakemake--a scalable bioinformatics workflow engine. Bioinformatics 28, 2520–2522. 10.1093/bioinformatics/bts480. [PubMed: 22908215]
64. Bolger AM, Lohse M, and Usadel B.(2014). Trimmomatic: a flexible trimmer for Illumina sequence data. Bioinformatics 30, 2114–2120. 10.1093/bioinformatics/btu170. [PubMed: 24695404]
65. Li D, Luo R, Liu CM, Leung CM, Ting HF, Sadakane K, Yamashita H, and Lam TW (2016). MEGAHIT v1.0: A fast and scalable metagenome assembler driven by advanced methodologies and community practices. Methods 102, 3–11. 10.1016/j.ymeth.2016.02.020. [PubMed: 27012178]
66. Huang X, and Madan A.(1999). CAP3: A DNA sequence assembly program. Genome Res 9, 868–877. 10.1101/gr.9.9.868. [PubMed: 10508846]
67. Robinson JT, Thorvaldsdottir H, Winckler W, Guttman M, Lander ES, Getz G, and Mesirov JP (2011). Integrative genomics viewer. Nat Biotechnol 29, 24–26. 10.1038/nbt.1754. [PubMed: 21221095]
68. Nishimura Y, Yoshida T, Kuronishi M, Uehara H, Ogata H, and Goto S.(2017). ViPTree: the viral proteomic tree server. Bioinformatics 33, 2379–2380. 10.1093/bioinformatics/btx157. [PubMed: 28379287]
69. Taylor LJ., Abbas A., and Bushman FD. (2020). grabseqs: simple downloading of reads and metadata from multiple next-generation sequencing data repositories. Bioinformatics 36, 3607–3609. 10.1093/bioinformatics/btaa167. [PubMed: 32154830]
70. Coordinators NR (2013). Database resources of the National Center for Biotechnology Information. Nucleic Acids Res 41, D8–D20. 10.1093/nar/gks1189. [PubMed: 23193264]
71. Langmead B, and Salzberg SL (2012). Fast gapped-read alignment with Bowtie 2. Nat Methods 9, 357–359. 10.1038/nmeth.1923. [PubMed: 22388286]
72. Li H, Handsaker B, Wysoker A, Fennell T, Ruan J, Homer N, Marth G, Abecasis G, Durbin R, and Genome Project Data Processing, S. (2009). The Sequence Alignment/Map format and SAMtools. Bioinformatics 25, 2078–2079. 10.1093/bioinformatics/btp352. [PubMed: 19505943]
73. Quinlan AR, and Hall IM (2010). BEDTools: a flexible suite of utilities for comparing genomic features. Bioinformatics 26, 841–842. 10.1093/bioinformatics/btq033. [PubMed: 20110278]

Highlights

- Redondoviruses are highly prevalent in human respiratory samples.
- Redondoviruses are associated with periodontitis, critical illness, and COVID-19.
- In human samples, redondoviruses co-occur with the amoeba *Entamoeba gingivalis*.
- Redondoviruses are found in *E. gingivalis* cultures, specifying amoebas as hosts.

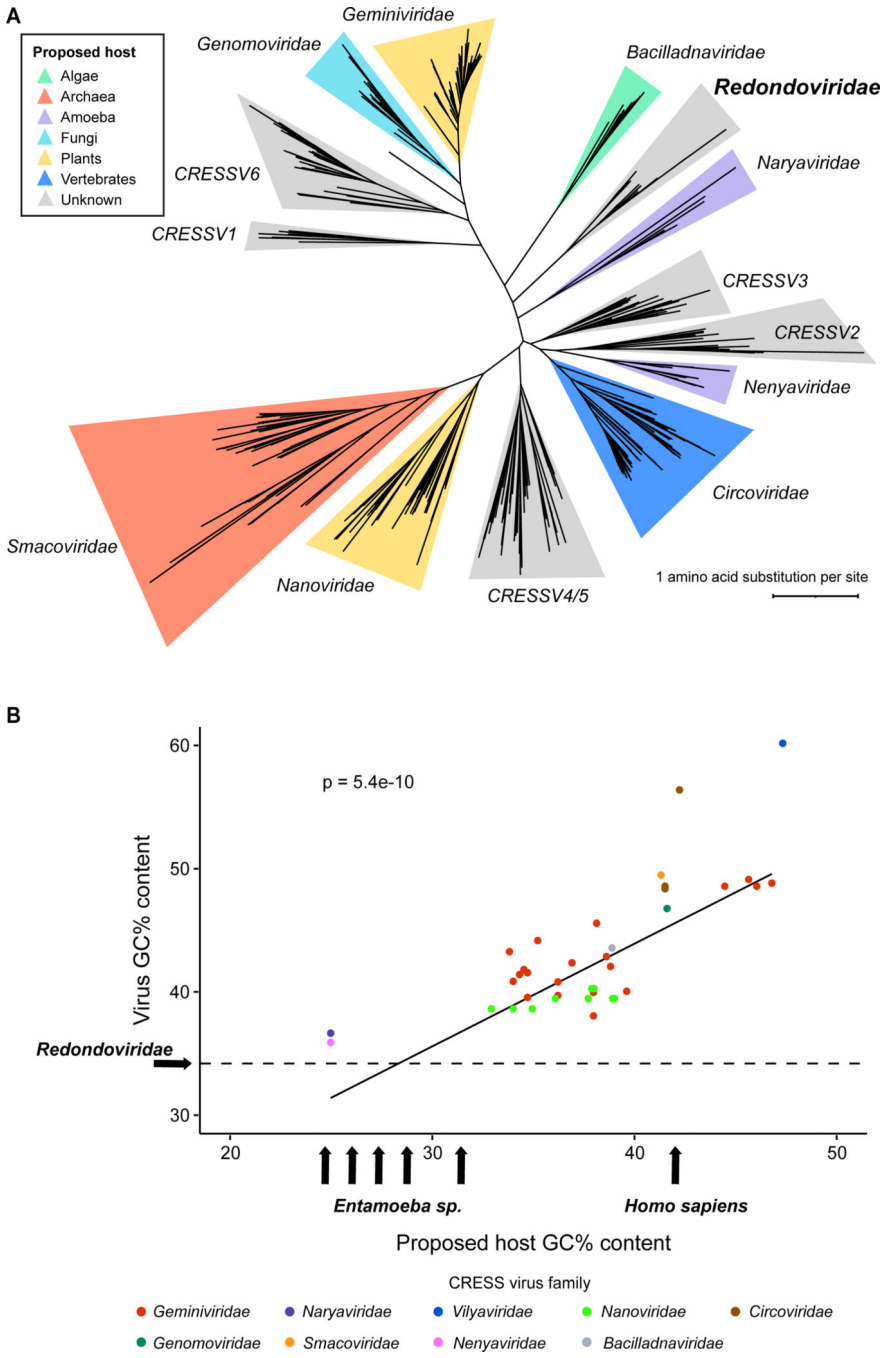

Figure 1.

Investigating the host cell supporting redondovirus replication. **(A)** Phylogenetic maximum-likelihood tree of Rep amino acid sequences from 441 members of the *Cressdnaviricota* phylum (Table S1). Rep sequences were aligned with MUSCLE[53], followed by tree construction using RaxML[54] and visualization using iTOL[55]. Clade coloring denotes the proposed host of the respective CRESS virus family. **(B)** Comparative analysis of GC content (% GC) of representative CRESS viruses and their hosts. Virus GC content positively correlates with host GC content ($R^2 = 0.63$, Pearson's Correlation Test p-value =

5.442e-10, n = 41). The *Entamoeba* arrows denote (from left to right): *E. dispar* (24.1%), *E. histolytica* (24.95%), *E. nuttalli* (25.1%), *E. moshkovskii* (26.5%), and *E. invadens* (30.3%). The dotted horizontal line represents the median GC content of *Redondoviridae* (34.25%). Figures adapted from Kinsella and coworkers [13].

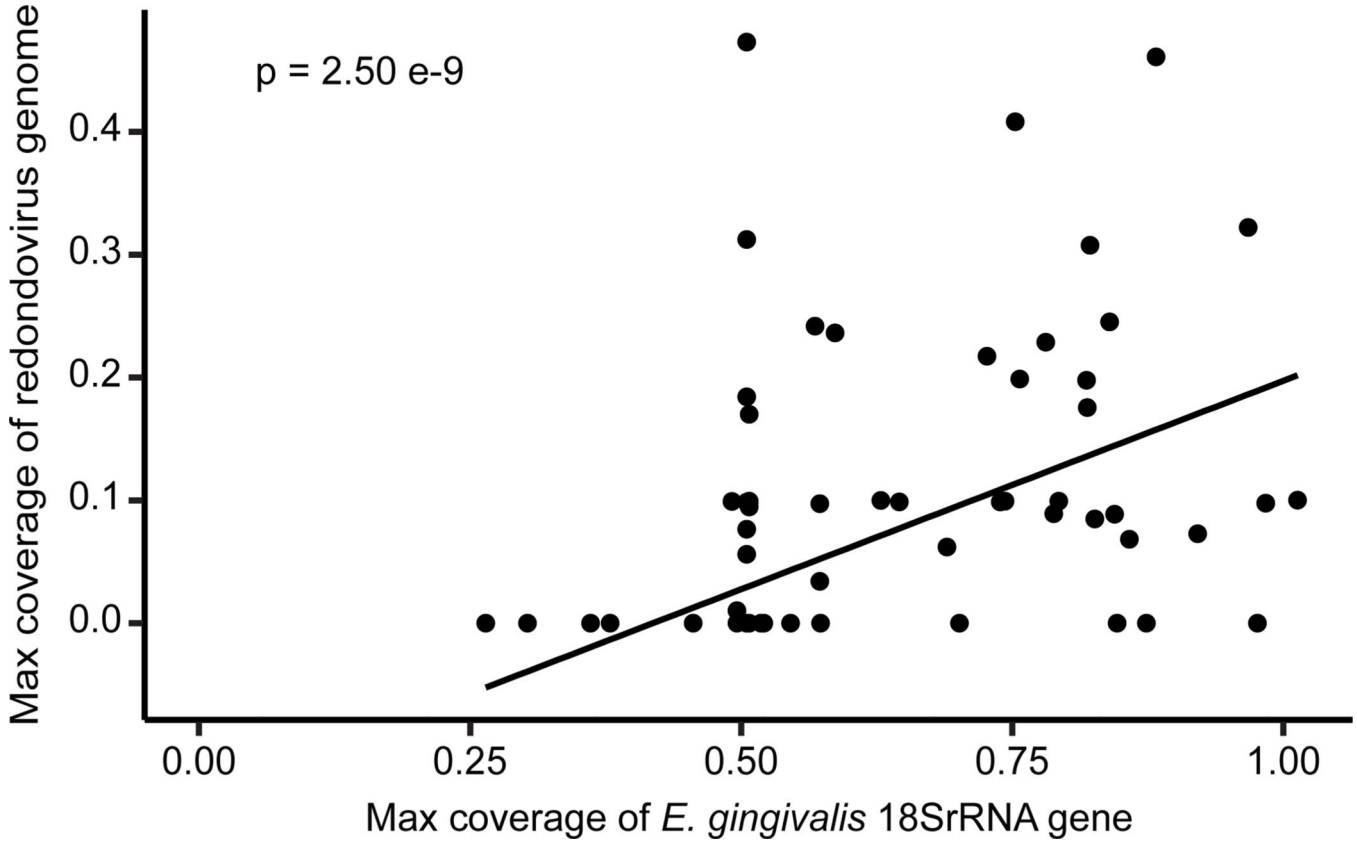

Figure 2.

Redondovirus and *E. gingivalis* abundance are positively associated in metagenomic DNA sequence data. Redondovirus relative abundance (measured using the maximum redondovirus genome coverage per sample) positively correlates with *E. gingivalis* relative abundance (measured using the maximum *E. gingivalis* 18S rRNA gene coverage per sample) in metagenomic data (NCBI BioProject IDs: PRJEB42701[17], PRJNA552294[18], PRJNA508385[18]) (R^2 = 0.49, Pearson's Correlation Test p-value = 2.501e-9, n = 130).

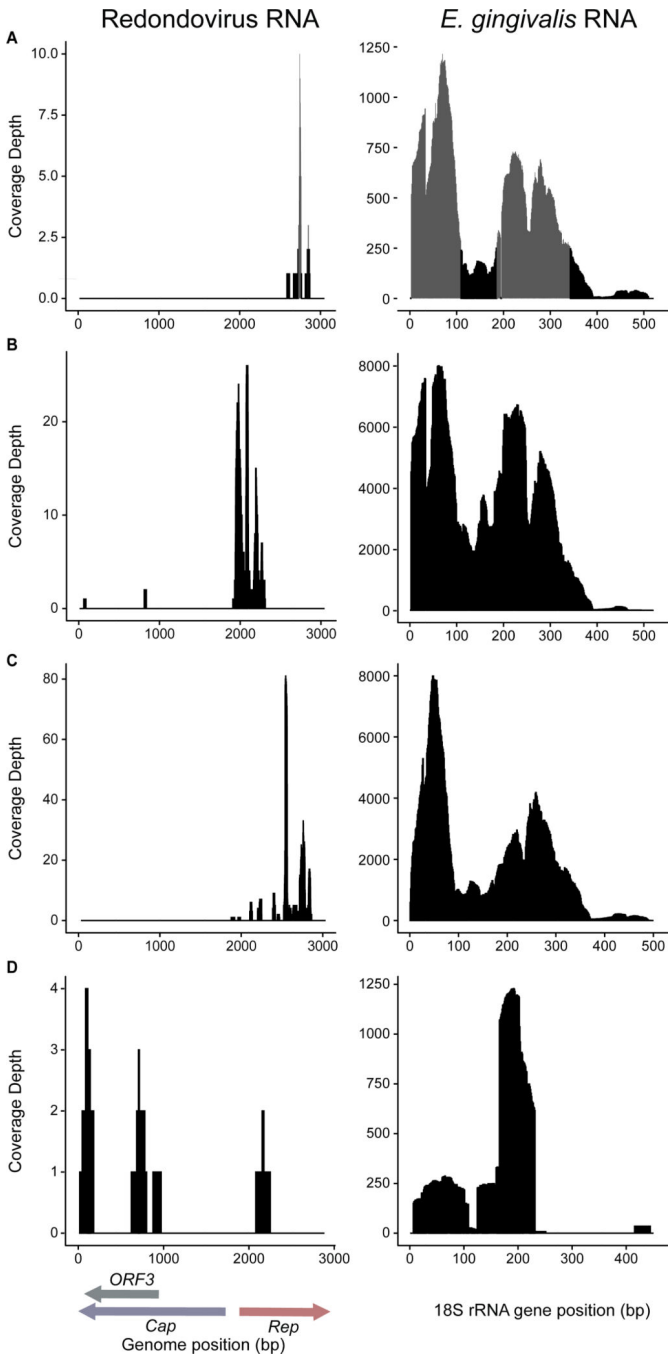

Figure 3.

Detection of redondovirus and *E. gingivalis* RNA in metatranscriptomic datasets. Alignments show RNA reads from two datasets derived from the gingival crevice of periodontitis patients (NCBI BioProject IDs: PRJNA221620[20], PRJNA319790[21]). Panels **(A)-(D)** represent individual samples from the datasets. The left side of each panel shows reads aligned to a redondovirus genome, with ORFs indicated at the bottom; the right side of each panel shows reads aligned to the *E. gingivalis* 18S rRNA gene. Panels **(A)-(C)** show samples from diseased gingival crevices of three patients sequenced

in PRJNA221620[20], and panel **(D)** shows pooled gingival tissues from periodontitis patients sequenced in PRJNA319790[21]. Plots were generated using the hisss pipeline (https://github.com/louiejtaylor/hisss). Query targets for alignment were **(A)** redondovirus NCBI accession MK059756.1 and *E. gingivalis* accession KX027290.1; **(B)** redondovirus NCBI accession MT482429.1 and *E. gingivalis* accession KX027290.1; **(C)** redondovirus accession MK059758.1 and *E. gingivalis* KX027293.1; **(D)** redondovirus accession MT482430.1 and *E. gingivalis* accession MG601094.1. Other samples from these datasets did not contain detectable redondovirus sequences and thus are not shown.

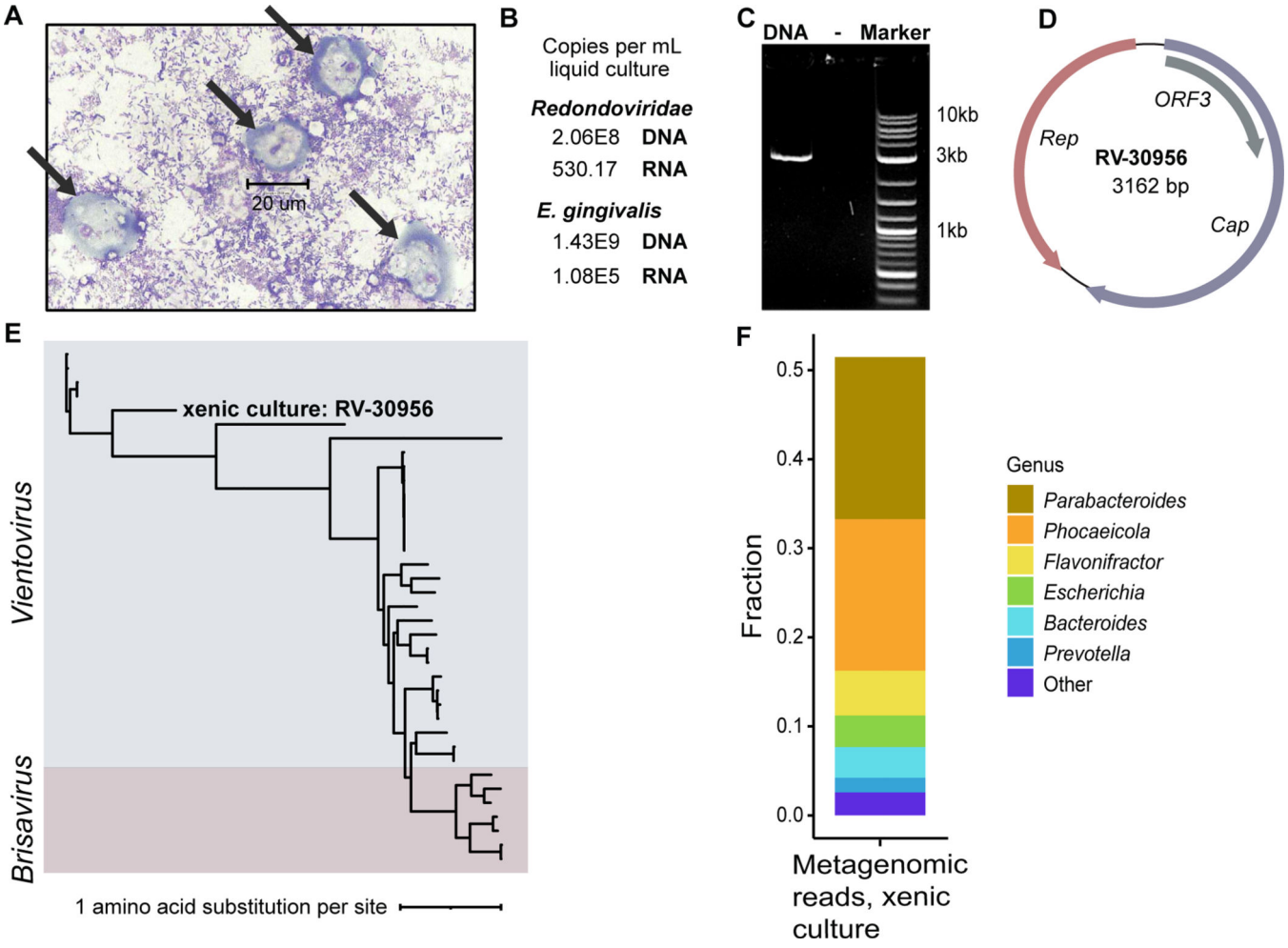

Figure 4.

Detection of redondovirus DNA and RNA in a xenic *E. gingivalis* culture. **(A)** Image of the xenic *E. gingivalis* culture *(*ATCC-30956) at 100X magnification stained using Kwik-Diff. Scale bar measures a cell (~20 um) that is morphologically consistent a *E. gingivalis* trophozoite (arrows). No cells with morphology expected for human cells were observed. **(B)** Detection of redondovirus and *E. gingivalis* DNA and RNA in the *E. gingivalis* culture by qPCR and RT-qPCR. **(C)** Agarose gel electrophoresis showing redondovirus genomic DNA amplification product of the expected size (~3 kb), generated by PCR of DNA from the xenic culture with “back-to-back” PCR primers targeting the circular redondovirus genome. **(D)** Genome map of the *Vientovirus* sequenced from the xenic *E. gingivalis* culture (RV-30956). The largest ORF (violet) encodes the putative capsid (Cap) protein, the second largest (salmon) encodes the Replication-associated (Rep) protein, and the third (grey) encodes a protein of unknown function (ORF3). **(E)** The RV-30956 sequence placed in a *Redondoviridae* phylogeny. Rep amino acid sequences from 37 redondoviruses were aligned with MUSCLE[53]. The tree was built using PhyML with branch support determined by approximate likelihood ratio test[56] and visualized using iTOL[55]. **(F)** Metagenomic sequence analysis of the *E. gingivalis* xenic culture. Taxa were identified using Kraken2[57] and BLASTn[58]. Only results with reads that could be assigned taxonomically are shown.

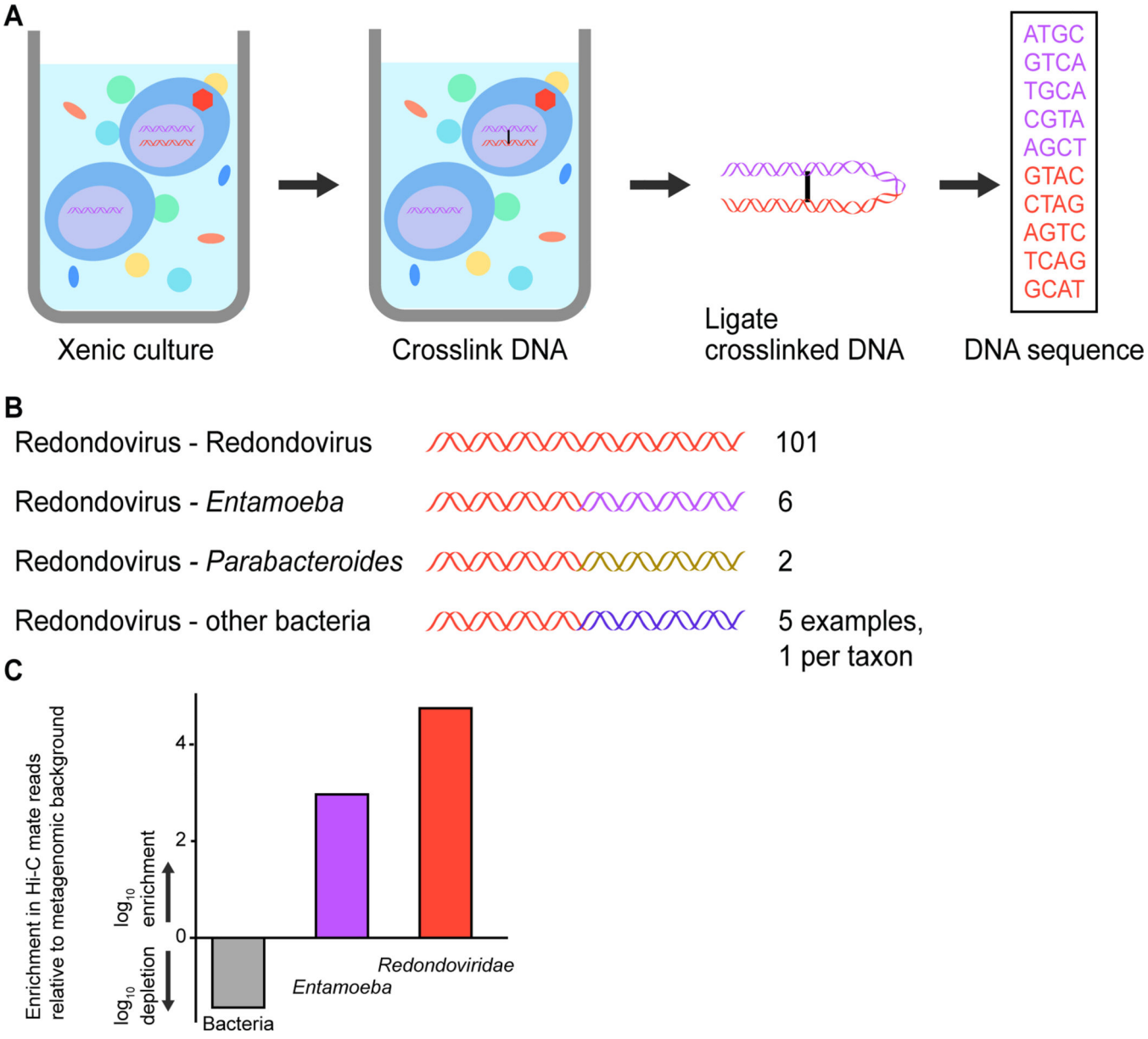

Figure 5.

Linking of redondovirus and *E. gingivalis* DNA in a xenic culture using DNA crosslinking and high-throughput sequencing (Hi-C). **(A)** Schematic diagram of the Hi-C chromatin conformation capture method (Phase Genomics). **(B)** Numbers of reads in cross-linked Hi-C pairs from the xenic culture where one read annotates as redondovirus, and the other annotates as redondovirus, *Entamoeba*, or bacteria. **(C)** Quantifying the degree of enrichment of *Entamoeba* reads among Hi-C reads linked to redondovirus sequences. The percentage of Hi-C reads linked to redondovirus mate pairs was compared to shotgun sequencing reads in total DNA from the xenic culture assigned to redondovirus, *Entamoeba*, and bacteria. Enrichment or depletion was determined by dividing the Hi-C percentage by the whole genome shotgun percentage and then applying a log10 transformation. Only 0.005% of total metagenomic reads in the culture could be identified as *Entamoeba*

sequences using BLASTn; in contrast *Parabacteroides* represented 20% of all identifiable metagenomic reads in the culture.

Table 1.

Co-occurrence of redondoviruses (RV) and *E. gingivalis* (EG) in human clinical specimens.

Subject status	Number of subjects	Sample type†	Redondovirus status	*E. gingivalis* status		p-value	Reference	Detection method
				EG+	EG-			
Peri-implantitis patients	41	Subgingival plaque	RV+ RV-	10 1	11 19	0.003626	Ghensi et al., 2020	Metagenomic sequencing
Mucositis patients	37	Subgingival plaque	RV+ RV-	7 1	4 25	0.0002265	Ghensi et al., 2020	Metagenomic sequencing
Healthy volunteers	35	Subgingival plaque	RV+ RV-	7 1	2 25	4.02E-5	Ghensi et al., 2020	Metagenomic sequencing
ICU patients	38	OP, NP, ETA	RV+ RV-	3 0	0 35	0.00012	Merenstein et al., 2021; this study	qPCR
COVID ICU patients	88	OP, NP, ETA	RV+ RV-	9 5	1 73	3.30E-8	Merenstein et al., 2021; this study	qPCR
Healthy volunteers	50	Saliva	RV+ RV-	15 7	1 27	9.85E-7	Taylor et al., 2021; this study	qPCR

†OP, oropharyngeal; NP, nasopharyngeal; ETA, endotracheal aspirate.

KEY RESOURCES TABLE

REAGENT or RESOURCE	SOURCE	IDENTIFIER
Biological samples		
Saliva samples from healthy humans	Taylor et al., 2021	N/A
Oropharyngeal, nasopharyngeal, and endotracheal aspirate samples subjects hospitalized with COVID-19	Merenstein et al., 2021	N/A
Oropharyngeal, nasopharyngeal, and endotracheal aspirate samples from medical intensive care unit patients	This study	N/A
Chemicals, peptides, and recombinant proteins		
Phi29 polymerase	New England BioLabs	Cat#M0269
Critical commercial assays		
TaqMan Fast Universal PCR Master Mix	Thermo Fisher	Cat#4352042
TaqMan Fast Virus 1-Step Master Mix	Thermo Fisher	Cat#5555532
PowerUp SYBR Green Mix	Thermo Fisher	Cat#A25741
DNeasy Blood and Tissue Kit	Qiagen	Cat#69504
QIAamp DNA Mini Kit	Qiagen	Cat#51304
SuperScript First-Strand Synthesis System Kit	Thermo Fisher	Cat#18080051
Scientific Kwik-Diff™ Staining Kit	Thermo Fisher	Cat#9990700
Phusion High-Fidelity PCR Kit	New England BioLabs	Cat#E0553S
Monarch DNA Gel Extraction Kit	New England BioLabs	Cat#T1020S
Nextera XT DNA Library Preparation Kit	Illumina	Cat#FC1311024
Deposited data		
Raw metagenomic sequencing reads	NCBI	Accession #: PRJNA858476
Raw shotgun sequencing reads	NCBI	Accession #: PRJNA858476
Redondovirus (RV-30956) genome	GenBank	Accession #: ON986208
Experimental models: Organisms/strains		
E. gingivalis	ATCC	ATCC-30956
Oligonucleotides		
qPCR, redondovirus *Cap* ORF (F: 5'-GGATGCCATGAAACTTTGATAC-3'; R: 5'TCTTCCTCCTTATTTGTATGGC-3'; probe: 5'-CCCATACTTACGCCGGTTACCTGC-3')	Integrated DNA Technologies	N/A
qPCR, *E. gingivalis* 18S rRNA gene (F: 5'-TACCATACAAGGAATAGCTTTGTGAATAA-3'; R: 5'-ACAATTGTAAATTTGTTCTTTTTCT-3')	Integrated DNA Technologies	N/A
Whole-genome PCR, redondovirus (Set A F: 5'CCTTTGGTCTCGAAATCTTCCTATACTGG-3'; Set A R: 5'-AGGCCTCTCTCCCTTCCATTTGG-3'; Set B F: 5'-GGTTATCGTTCATTTGATCATGCATTAGTACC-3'; Set B R: 5'-ACCAAGATGTTTAAGCCCTTTAGTTAATGTTTC-3')	Integrated DNA Technologies	N/A
qPCR, human GAPDH (F: 5'-GGTGGTCTCCTCTGACTTCAACA-3'; R: 5'CCAGCCACATACCAGGAAATG-3'; probe: 5'CTGGCATTGCCCTCAACGACCAC-3')	Integrated DNA Technologies	N/A
Recombinant DNA		
pUC57	BioBasic	Addgene 4509

REAGENT or RESOURCE	SOURCE	IDENTIFIER
Software and algorithms		
BLASTn v2.9.0	Altschul et al., 1990	https://www.ncbi.nlm.nih.gov/books/NBK279690/
PhyML v3.0	Guindon et al., 2010	https://github.com/stephaneguindon/phyml
RaxML v8.2	Stamatakis et al., 2005	https://github.com/stamatak/standard-RAxML
MUSCLE v3.8.31	Edgar, 2004	https://github.com/rcedgar/muscle
iTOL v6	Letunic and Bork, 2019	https://itol.embl.de/
VipTree v3.1	Nishimura et al., 2017	https://www.genome.jp/viptree/
hisss v3.0	Abbas et al., 2019	https://github.com/louiejtaylor/hisss
IGV v2.9.0	Robinson et al., 2011	https://software.broadinstitute.org/software/igv/
CAP3 v3.0	Huang and Madan, 1999	http://doua.prabi.fr/software/cap3
MEGAHIT v1.2.9	Li et al., 2015	https://github.com/voutcn/megahit
FastQC v0.11.9	Andrews, 2010	https://github.com/s-andrews/FastQC
Trimmomatic v0.39	Bolger et al., 2014	https://github.com/usadellab/Trimmomatic
Sunbeam v2.1.0	Clarke et al., 2019	https://github.com/sunbeam-labs/sunbeam
Kraken2 v2.1.2	Wood et al., 2019	https://github.com/DerrickWood/kraken2
R version v4.0.4	Ihaka and Gentleman, 1996	https://www.r-project.org/
Snakemake v7.16.0	Köster and Rahmann, 2012	https://github.com/snakemake/snakemake
SAMtools v1.9	Li et al., 2009	http://samtools.sourceforge.net/
BEDtools v2.30.0	Quinlan and Hall, 2010	https://bedtools.readthedocs.io/en/latest/